Lawrence Berkeley National Laboratory
Lawrence Berkeley National Laboratory

Title
ELECTRICAL PROPERTIES OF DISLOCATIONS IN ULTRA-PURE GERMANIUM

Permalink
https://escholarship.org/uc/item/4cd8b6qv

Author
Hubbard, G. Scott

Publication Date
1979-06-01

Peer reviewed

eScholarship.org Powered by the California Digital Library
University of California

MASTER

LBL-9342

Lawrence Berkeley Laboratory

UNIVERSITY OF CALIFORNIA, BERKELEY

Engineering & Technical Services Division

Presented at the 21st Electronic Materials Conference, Boulder, CO, June 27-29, 1979 and to be published in the Journal of Electronic Materials, Volume 9.

ELECTRICAL PROPERTIES OF DISLOCATIONS IN ULTRA-PURE GERMANIUM

G. Scott Hubbard and Eugene E. Haller

June 1979

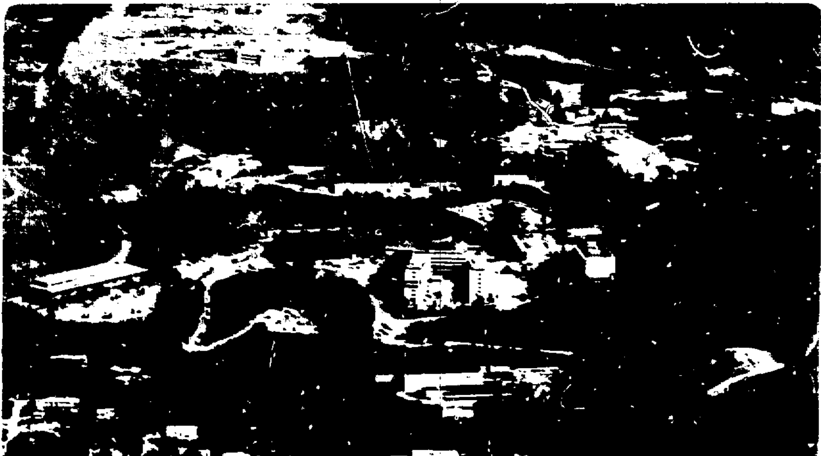

Prepared for the U.S. Department of Energy under Contract W-7405-ENG-48

Presented at the 21st Electronic Materials
Conference, Boulder, Colorado, June 1979.
To be published in Journal of Electronic
Materials, Volume 9.

LBL-9342

MASTER

ELECTRICAL PROPERTIES OF DISLOCATIONS IN ULTRA-PURE GERMANIUM

G. Scott Hubbard and Eugene E. Haller

June 1979

Lawrence Berkeley Laboratory
University of California
Berkeley, California 94720

ELECTRICAL PROPERTIES OF DISLOCATIONS* IN ULTRA-PURE GERMANIUM

G. Scott Hubbard and Eugene E. Haller

Lawrence Berkeley Laboratory
University of California
Berkeley, California 94720 U.S.A.

Abstract

Defect states due to grown-in dislocations in ultra-pure p-type germanium have been observed using Deep Level Transient Spectroscopy (DLTS) and Hall effect. These states are found to be composed of two bands of acceptor type levels whose energy and half width are influenced by both the presence of hydrogen and the crystal growth direction. At a net acceptor concentration of 10^{10} cm^{-3} a threshold dislocation density of 10^4 cm^{-2} is required for the observation of dislocation bands.

Introduction

The need for large volume, high resolution photon and charged-particle detectors which can be handled and stored at room temperature or higher has led to the development of ultra-pure germanium [(N_A-N_D) 2×10^{10} cm^{-3}] in our laboratory and elsewhere (1,2). Single crystals grown by the Czochralski method in [111], [100] and [113] directions in H_2, N_2 (1 atm) and in a vacuum of 10^{-6} Torr, have been produced in the course of this work. The dislocation density in these crystals, as revealed by preferential etching, may range from 0 to 10^5 cm^{-2}. Ultra-pure germanium suitable for detector fabrication typically contains 10^2 - 10^3 dislocations cm^{-2}.

---

*This work was supported by the Division of Physical Research of the U. S. Department of Energy under Contract No. W-7405-ENG-48.

The energy resolution of detectors made from this germanium is sometimes worse than expected from charge production statistics and electronic noise (3). This degradation in resolution, characterized by asymmetric and/or broadened peaks, has been correlated with a number of lattice defects including dislocations. It has been shown by Glasow and Haller (4) that when the dislocation density exceeds 10^4 cm^{-2} the full width half maximum (FWHM) of a spectral line increases rapidly. Such a marked influence of grown-in dislocations on device performance has led us to further investigate the electrical properties of these defects in ultra-pure germanium.

While the electrical properties of dislocations induced in germanium by plastic deformation have been examined experimentally for some time (5-7), little is known about the electrical properties of dislocations in undeformed germanium. The reasons grown-in dislocations have not been examined are twofold: (1) By twisting or bending the crystal, dislocations of mainly one type (e.g., edge, 60° or screw) can be created, thus rendering the experiment more amenable to theoretical modeling. During the process of crystal growth, there is no way to control the type of dislocations which occur. (2) Large numbers of dislocations (EPD ~ 10^7-10^8 cm^{-2}) made by deforming the crystal were needed to create an electrical effect which could be detected above the chemical impurity background in the germanium used [$|N_A-N_D|$ ~ 10^{12}-10^{13} cm^{-3}]. In the present study, the low concentrations of chemical impurities has enabled us to examine the electrical effects of fewer than 10^4 dislocations cm^{-2}.

Experimental Techniques

Preferential Etching

The samples used for dislocation counting were first cut perpendicular to the axis of crystal growth (either [100] or [113]), lapped with 600 and 1900 grit lapping compound and then polish-etched in a 7:2:1 mixture of HNO_3, HF and red fuming HNO_3. Dislocations were then decorated by means of a preferential etchant. For [100] samples, a one minute etch with a mixture of $CuNO_3$(10%):HNO_3:HF (1:1:2) was used. Revealing etch pits on the [113] plane required 6-10 minutes in a solution of $CuNO_3$(10%):H_2O_2:HF (1:1:2) as described elsewhere (8). The average etch pit size tends to be much smaller for [113] dislocations, accounting for a different appearance in photographs (see Figures 1 and 5).

Early work by Vogel (20) established that certain rows of etch pits in germanium revealed by preferential etching were due to purely edge dislocations which formed a lineage or low angle grain boundary.* Vogel assumed that other "isolated" etch pits were also edge dislocations, although this has not been proven. Preliminary observations using x-ray topography techniques on [100] crystals grown in our laboratory suggest that individual grown-in dislocations of many different types may be found in the same crystal slice (19). We also observe lineages in our samples as described by Vogel and assume that they are made up of edge dislocations.

Hall Effect

Variable temperature Hall effect measurements were made on p-type slices over the temperature range 5K to 300K. Samples were cut to a size of

---

*We will follow the generally accepted terminology that defines a lineage as any low angle grain boundary where the degree of misfit is $< 1°$ (9).

approximately 1 cm x 1 cm x 2mm, lapped and polish etched as described in the previous section. Ohmic contacts were made by indium solder applied to the four corners, yielding a Van der Pauw geometry (10). A magnetic field of 6000 gauss was used in the temperature range 300K to 77K while a field of 1200 gauss was applied below 77K. Low field corrections due to magnetoresistance effects were thereby minimized. Temperature measurements were taken using a silicon diode thermometer (11) which can be used over a temperature range of 4K to 300K, thus eliminating the need to switch between sensors.

Deep Level Transient Spectroscopy (DLTS)

Deep Level Transient Spectroscopy using the correlator technique described by Miller et al (12), was also employed to examine the electrical effects of dislocations. Details of our experimental set-up can be found elsewhere (13). All the diodes used in this work were p-type and were fabricated with Li-diffused n^+-contacts and ^{11}B ion-implanted p^+-contacts. Each diode had a surface area of a few cm^2 and was about 3mm thick in order to maintain a similar capacitance from sample to sample. Unless stated otherwise, all spectra discussed in this paper were taken with a correlator time constant of 3 msec. The power of this technique lies in its spectroscopic nature. While the Hall effect gives the concentration and mobility of various impurities in an unambiguous fashion, determination of energy levels, particularly those close to the middle of the forbidden band, can be quite difficult. With DLTS the presence of a peak for a given deep impurity makes activation energy measurement more precise.

Electrical Properties of Grown-In Dislocations

Dislocation Density

Earlier work with many detectors having differing etch pit densities (EPD) had already suggested that at an EPD = 10^4 cm^{-2}, dislocations caused pronounced electrical effects. Accordingly, we elected to study crystals in which the EPD increased from a few thousand to ~ 10^4 cm^{-2} in a short distance along the length of a crystal so that the concentration of shallow impurities would be nearly constant. An example is shown in Figure 1, DLTS spectra for three nearby samples of differing dislocation density were taken using the same experimental conditions for each sample. Below an EPD of ≃ 10^3 cm^{-2}, dislocations in as-grown crystals are usually widely separated (sometimes > 1mm) and randomly scattered. DLTS spectra of these low EPD samples show no features correlated with dislocations under even the most sensitive conditions.* At an EPD of about 5 x 10^3 cm^{-2}, as shown by 281-6.5(1), some dislocations begin to cluster and a broad, small peak appears in the DLTS spectrum at ~ 23K. As the dislocation density increases, more clustering occurs and the peak becomes more pronounced as shown by sample 281-6.5(2). Microscopic examination revealed that nearest neighbor distances in the etch pit clusters are on the order of 25 μm. It is not clear whether this clustering is due to the multiplication of previously isolated dislocations or some driving force.

At an average EPD of 15 x 10^3 cm^{-2} virtually all dislocations appear to form short lineages where nearest neighbors are about 15 μm away, as demonstrated by sample 281-7.6(2). Now the peak (labeled -b-) is very large,

---

*In the spectra shown, the signal to noise ratio is ~ 100:1.

with a maximum at 22.4K. The natural line width (ΔT) of a single defect state is ~0.14T where T is the temperature at the peak position. Peak -b- has a half-width of 11K, which is 3.5 times the natural line width. Following the approach of Kimerling (21), we will express the bandwidth of the dislocation related defect as 3.5 k ΔT (or 0.95 meV) in this case. By plotting the dislocation peak position as a function of the correlator time constant an activation energy of E_V + 0.02 eV was determined.

There is a smaller feature in the spectra (labeled -a-) which extends to much higher temperatures and accompanies the -b- peak. The -a- peak bandwidth may be as much as 10 times that of a peak due to a single energy level. This evidence suggests that the dislocations give rise to two series or bands of levels.

The Hall effect data (Figure 2) for sample 281-7.6 shows features which compare directly with the DLTS spectra. Deionizing from 77K to 30K (-a- in Figure 2) appear to be distributed levels with a total concentration of 5×10^9 cm^{-3}. Since the temperature range over which this level deionizes is very similar to the small broad peak (also labeled -a-) in Figure 1, we believe they are due to the same defect. Measurement of the freeze out slope of feature -a- yields an activation energy of E_V + 0.014 eV which is at variance with the temperature at which the levels appear. From the point at which 50% of the levels are deionized, an energy of E_V + 0.08 eV is calculated. Similarly, the feature -b-, which freezes out between 30K and 20K, has an activation energy of E_V + 0.02 eV when the slope is measured and an energy of E_V + 0.04 eV when the temperature of 50% carrier freeze out is considered. Over nearly the same temperature range we observed peak -b- in Figure 1 which also had an apparent activation energy of 20 meV, suggesting that the same defect has been measured by both techniques. Since no other deep chemical acceptors were found by either method, the evidence indicates

that grown-in dislocation densities of ~ 10^4 cm^{-2} give rise to two distinct bands of acceptor type levels in ultra-pure germanium.

Crystal Growth Ambient

An empirical observation of high-purity germanium crystal growth has been that only those crystals grown in an atmosphere of pure H_2 are consistently free from charge trapping and thus usable for detector fabrication. This observation has led us to discover numerous instances where hydrogen plays an electrically active role in the germanium lattice as a component of various impurity complexes like divacancy-hydrogen (V_2), copper-hydrogen (CuH) and others (14,15,22).

Figure 3 shows DLTS measurements comparing two crystals, one grown in H_2 and the other N_2. Sample 135-17.5(2) has EPD ~ 10^3 cm^{-2} and contains the chemical impurity copper which has three acceptor levels, one of which appears near 20K (E_V + 0.04 eV). No trace of any band of levels related to dislocations could be found. In another part of the same slice where the EPD ~ 10^4 cm^{-2} [135-17.5(1)*], two very broad dislocation bands appear in addition to the copper peak. By comparison with a sample grown in H_2 with similar EPD [281-7.6 (1)] the dislocation bands in N_2 grown crystals are much broader. In fact, the feature at -b- has a very nearly flat top and FWHM of 8.4 k ΔT (2.7 meV). As with the crystal grown in H_2, there appears a second dislocation band, -c-, which extends to higher temperatures than the corresponding band in the H_2 crystal.

---

*At times during the growth of germanium crystals, the dislocation density will increase non-uniformly so that it is possible to have both high and low EPD on one slice cut perpendicular to the growth axis.

Hall effect measurements of low EPD (10^3 cm^{-2}) and high EPD ($\geq 10^4$ cm^{-2}) sections of one slice from a crystal grown in nitrogen are given in Figure 4. The low EPD section [136-11.9(2)] has only one deep chemical acceptor, Cu^0 at E_V + 0.04. In the high EPD sample [136-11.9(1)], the presence of many dislocations introduces a series of distributed levels. These levels first appear at a much higher temperature than those seen in the crystal grown in hydrogen (Figure 2). At 60K the carrier concentration of the high EPD sample has dropped below that of 136-11.9(2). It is possible but very unlikely that the shallow impurity concentration differs in the two sections of the crystal. It is more likely that we are observing the donor behavior of dislocations as described by Schröter (23).

Crystal Growth Direction

Following a suggestion for compound semiconductor crystal production (16), we have grown germanium crystals in the [113] direction in an attempt to improve the crystallography. It was found subsequently that detectors made from crystals grown in the [113] direction which had EPD $\geq 10^4$ cm^{-2} did not show the same charge trapping characteristics as did [100] crystals with similar EPD (17). This observation suggested that we examine the effects of crystal growth direction on dislocation bands as shown in Figure 5. Comparing [100] and [113] crystals with similar EPD demonstrates that the dislocation bands in the [113] crystal are shifted down in temperature and are reduced in activation energy relative to those appearing in the [100] crystal. The activation energy of the principal dislocation peak at 20K in crystal 499-9.4 is E_V + 0.015 eV compared to E_V + 0.02 eV for 281-7.6. The small bump at 41K is a level at E_V + 0.07 eV which appears often and may be due to some impurity complex involving copper and oxygen.

Discussion and Summary

The use of ultra-pure germanium with varying dislocation densities as an experimental medium for the study of the electrical effects of dislocations has elucidated some new properties of dislocations. The bands of levels associated with dislocations in germanium are not observed until the dislocations reach a critical density ($\sim 10^4$ cm^{-2}). This apparent threshold effect is at odds with the theoretical models (5-7) where isolated dislocations* give rise to energy bands in the forbidden gap. A simple calculation, which assumes 10% of the dangling bonds to have accepted an electron, yields an acceptor concentration of 3.5×10^9 cm^{-3} for 10^3 dislocations cm^{-2}. In p-type samples, where the chemical impurity concentration is $\sim 10^{10}$ cm^{-3}, the acceptors due to 10^3 dislocations should be easily seen by both DLTS and Hall effect but in fact are not observed. However, it may be that when the dislocation density is small (10^3 cm^{-2}) the concentration of defect states is simply too low to be seen with our current procedures. At present, we cannot clearly distinguish between a threshold effect due to clustering of dislocations and the lower limit of our instrumental sensitivity.

Hydrogen appears to play a role in modifying the width and position of these dislocation bands as shown in the comparison of N_2 and H_2 grown crystals. The difference suggests that hydrogen changes the activation energy of these defects by saturating the dangling bands which are present at complete dislocations. An alternate explanation might be found in the recent observation that the number and energy of multiple acceptors in germanium (e.g., Cu) are both reduced in the presence of hydrogen (14).

---

*These models specify a single dislocation line propagating along the growth axis of the crystal. This would be observed as a single etch pit on a slice cut perpendicular to the growth axis.

The direction of crystal growth also seems to influence dislocation associated defect states. Although the shape and width of the dislocation band in the [113] crystal is similar to that of the [100] crystals, the principal features are shallower in energy. Since Hornstra (18) demonstrated that many different types of dislocations are possible, it may be that by growing the crystal in a different direction the dislocation geometry is such as to reduce the extent of the strain fields surrounding the dislocations and thereby modify the dislocation band structure. This effect is important in device applications since it is the moderately deep traps which have time constants for carrier trapping and detrapping that most affect our radiation detector spectra. By growing crystals in a [113] orientation, and thus making dislocation defect states shallower in energy, we reduce the contribution of dislocation density to charge trapping.

Acknowledgements

We wish to acknowledge the continued support and encouragement of F. S. Goulding and thank W. L. Hansen for many useful discussions.

References

1. R. N. Hall, IEEE Trans. Nucl. Sci. NS-21, 260 (1974).

2. W. L. Hansen and E. E. Haller, IEEE Trans. Nucl. Sci. NS-21, 251 (1974).

3. W. L. Hansen, R. H. Pehl, E. J. Rivet and F. S. Goulding, Nucl. Inst. and Methods, 80, 181-186 (1970).

4. P. A. Glasow and E. E. Haller, IEEE Trans. Nucl. Sci. NS-23, 92 (1976).

5. W. T. Read, Phil. Mag. 45, 775, (1954).

6. W. Schröter and R. Labusch, Phys. Stat. Sol. 36, (1969).

7. S. Marklund, Phys. Stat. Sol. 85, 673 (1978).

8. E. E. Haller and W. L. Hansen, Lawrence Berkeley Laboratory report LBL-1744, March, 1973.

9. H. F. Matare, Defect Electronics in Semiconductors, Wiley Interscience, New York (1971).

10. L. J. *Van der Pauw*, Philips Res. Rep. 13, 1 (1958).

11. Lake Shore Cryotronics, Model DT-500P-GR-M, 64 E. Walnut St., Westerville, Ohio 43081.

12. G. L. Miller D. V. Lang and L. C. Kimerling, Ann. Rev. of Material Sci. 377 (1977).

13. E. E. Haller, P. P. Li, G. S. Hubbard and W. L. Hansen, IEEE Trans. Nucl. Sci. NS-26, No. 1 (February 1979).

14. W. L. Hansen and E. E. Haller, IEEE Trans. Nucl. Sci. NS-19, 260 (1972).

15. E. E. Haller, G. S. Hubbard and W. L. Hansen, IEEE Trans. Nucl. Sci. NS-24, 48 (1977).

16. R. C. Sangster, Compound Semiconductors, Vol. 1, Ch. 28, pp. 241-253, Reinhold Publishing Corp., New York (1962).

17. G. S. Hubbard, E. E. Haller, and W. L. Hansen, IEE Trans. Nucl. Sci. NS-26, No. 1 (1979).

18. J. Hornstra, J. Phys. Chem. Solids 5, 129 (1958).

19. W. Oppolzer, Private Communication, Siemens R&D Laboratories, Munich.

20. F. L. Vogel, Jr., Acta Metallurgica 3, 245 (1955).

21. L. C. Kimerling and J. R. Patel, App. Phys. Lett. 34, 73 (1979).

22. E. E. Haller, Inst. of Phys. Conf. Series No. 46, p. 205-211, London (1979).

23. W. Schröter, Inst. of Phys. Conf. Series No. 46, p. 114, 127, London (1979).

Figure Captions

Figure 1. Capacitive transient spectra of defect states associated with increasing dislocation density in germanium crystal 281 (grown in the [100] direction under 1 atm of H_2). Nearest neighbor distance between etch pits in picture 2 is 25 μm, in picture 3, 15 μm (microphotographs taken at 50x). Below EPD = 5×10^3 cm^{-2} no spectroscopic features could be seen. Activation energy of peak -b- is $E_V + 0.02$ eV, half width ($k\,\Delta T$) is 0.35 meV. Half width of -a- is ≈ 2 meV ($k\,\Delta T$). $(N_A - N_D) \sim 1 \times 10^{10}$ cm^{-3}, τ_R = 3 msec.

Figure 2. Hole concentration in sample 281-7.6 (EPD = 15×10^3 cm^{-2}) as a function of 1000/T (K). The acceptor levels deionizing in region -a- and -b- are correlated with high dislocation density and seem to be the same as peaks -a- and -b- in Figure 1. Concentration of -a- is 5.0×10^9 cm^{-3}, -b- = 4.1×10^9 cm^{-3}. The slope of the carrier freeze-out gives an activation energy of $E_V + 0.014$ eV for -a- and $E_V + 0.02$ eV for -b-. The temperature at which 50% of the levels are deionized yields an energy of 0.08 eV for -a- and 0.04 eV for -b-.

Figure 3. Capacitive transient spectra of defect states associated with EPD $\geq 10^4$ cm^{-2} for crystals grown in H_2 (281) and N_2 [135-17.5(1)] EPD of sample 135-17.5(2) is 10^3 cm^{-2}. The peak labeled -a- at 21K is Cu^0 at $E_V + 0.04$ eV. Dislocation related features are -b- and -c- in sample 135-17.5(1). The bandwidth of -b- is 2.7 meV ($k\,\Delta T$) while -c- is ≈ 2 meV. Sample 281-7.6(1) is similar to samples in Figure 1. τ_R = 30 msec.

Figure 4. Hole concentration as measured by Hall effect is shown as a function of 1000/T (K) for a crystal grown in N_2 (136). Sample 136-11.9(2) has EPD = 10^3 cm^{-2} and shows only one level: Cu^0 at $E_V + 0.04$ eV. Sample 136-11.9(1) has EPD > 10^4 cm^{-2} and shows defect states from 200K to < 16K. From the temperature at which 50% of the states are deionized, the calculated activation energy is $E_V + 0.2$ eV.

Figure 5. Capacitive transient spectra comparing the defect states due to dislocation densities 10^4 cm^{-2} for crystals grown in the [100] and [113] directions. Microphotograph of etch pits taken at 50x. From the peak position as a function of time constant we deduce an activation energy of E_V + 0.015 eV for sample 499-9.4. τ_R = 3 msec.

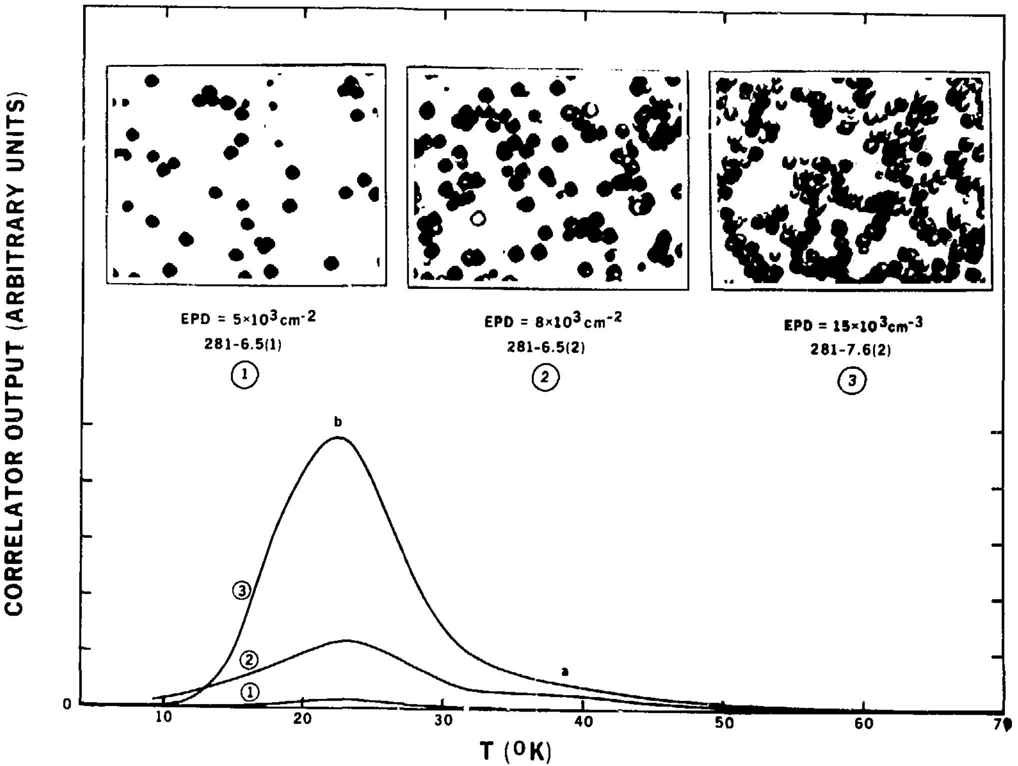

Figure 1

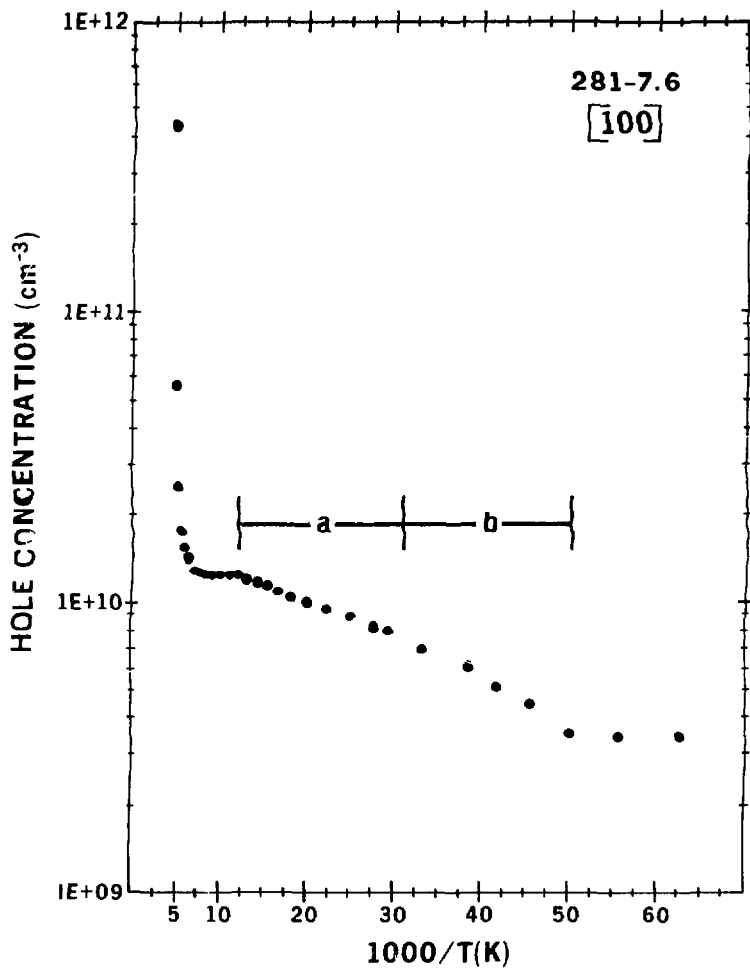

XBL 789-10906

Figure 2

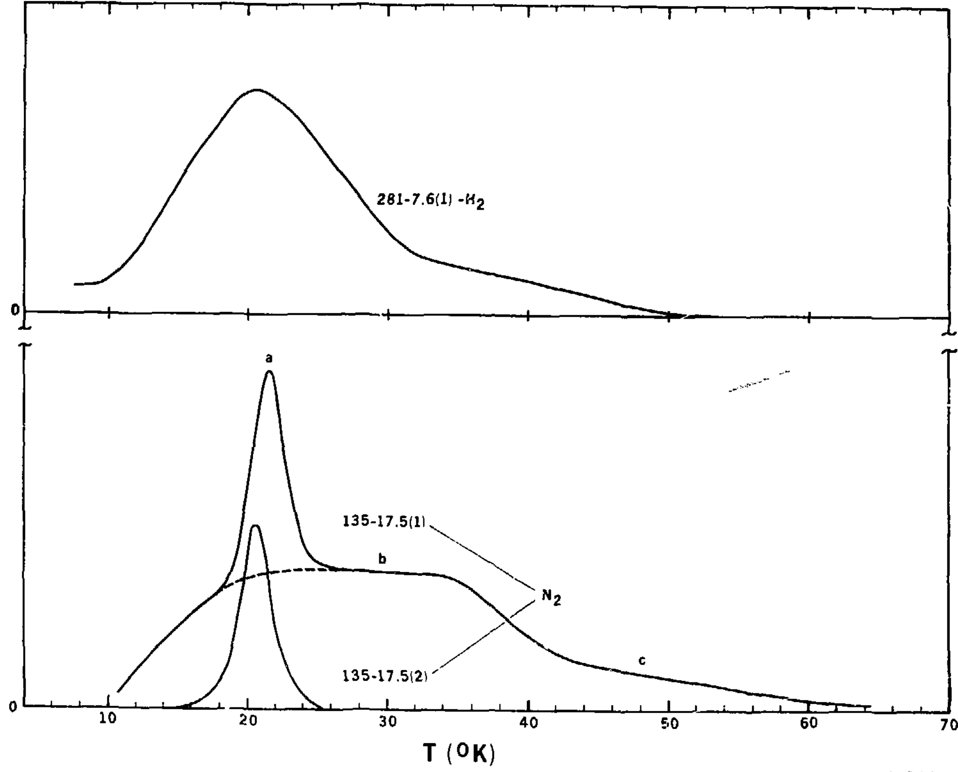

Figure 3

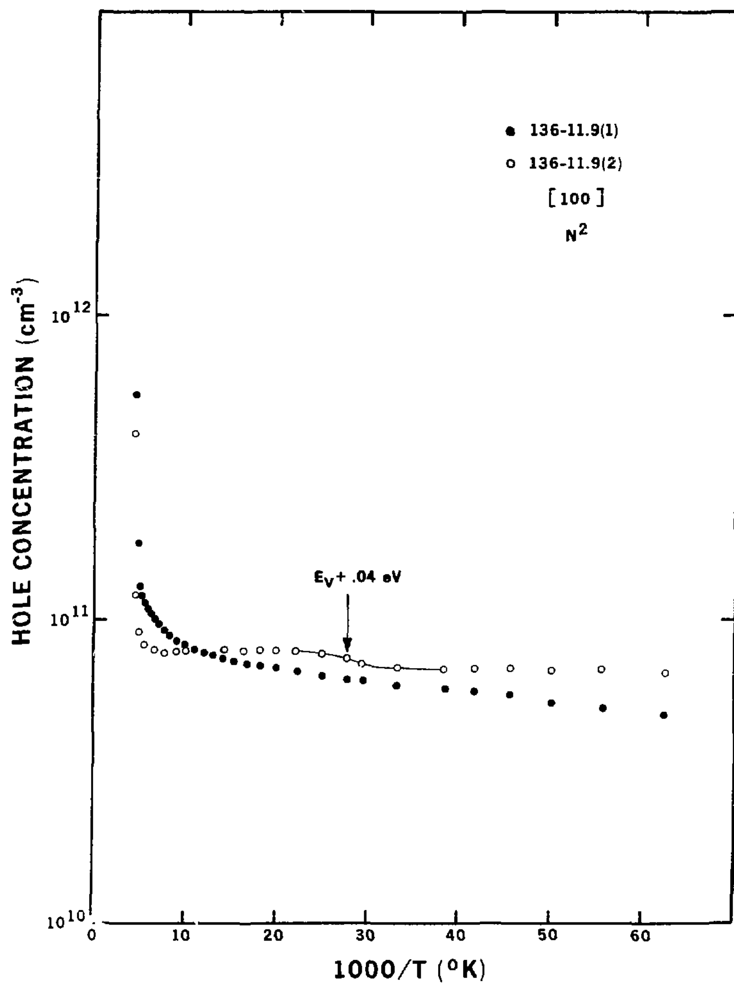

XBL 796-10205

Figure 4

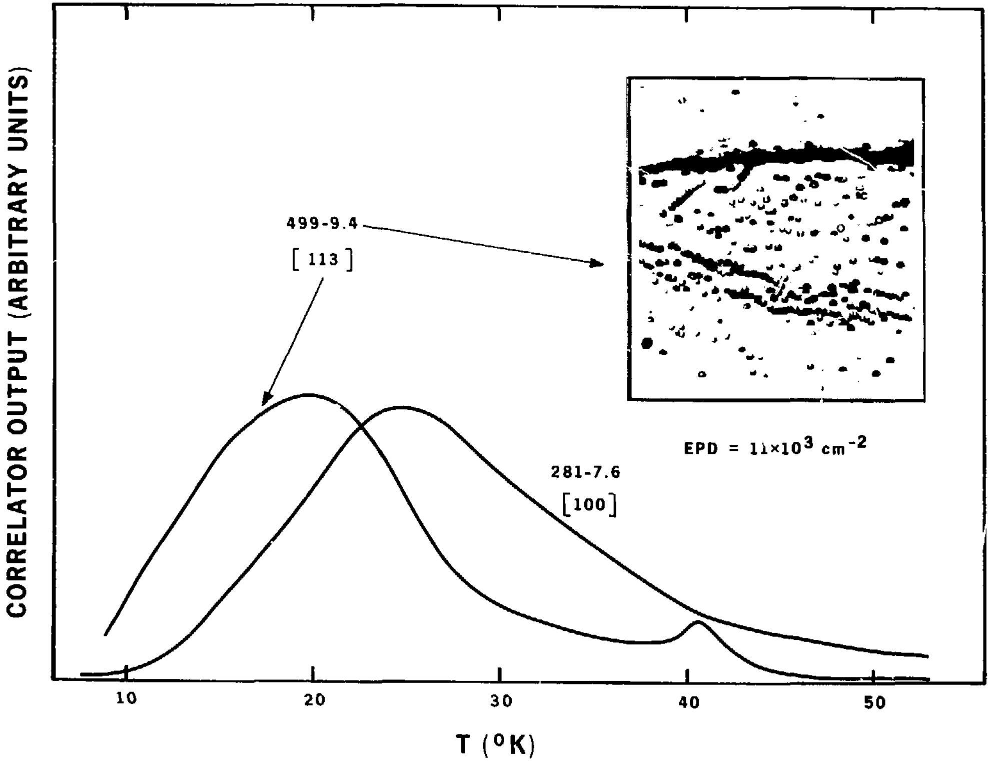

Figure 5